

Synchrotron radiation-stimulated photochemical reaction and its application to semiconductor processes

Tsuneo Urisu, Jun-ichi Takahashi, Yuichi Utsumi and Housei Akazawa
NTT LSI Laboratories, 3-1 Morinosato Wakamiya, Atsugi-shi, Kanagawa Pref. 243-01, Japan

Recent results are reviewed on synchrotron radiation (SR)-excited photochemical reaction studies aimed at applications to semiconductor processes. Valence or core electronic excitations induced by SR irradiation and ensuing chemical reactions are classified and characterized by rate equations. Unique material selectivity in etching has been found. SiO₂ has been found to evaporate by SR irradiation and this phenomenon can be applied to the low-temperature surface cleaning of silicon. In the epitaxial growth of Silicon by ultrahigh-vacuum chemical vapor deposition using Si₂H₆, SR irradiation significantly lowers growth temperature beyond the low-temperature limit of thermal reaction. Lowering of the operating temperature by SR irradiation is especially effective in applications to the atomic layer epitaxial growth of silicon. The layer-by-layer process has been successfully demonstrated, confirming self-limiting adsorption of SiH₂Cl₂ and ensuring surface reactivation by SR irradiation.

Keywords: Synchrotron radiation, photochemical reaction, semiconductor process, etching, chemical vapor deposition, epitaxial growth, atomic layer epitaxial growth

1 INTRODUCTION

Synchrotron radiation (SR) is intense and stable light covering the wide energy range from hard X-ray to infrared, and is used in many scientific and engineering fields. The photochemical semiconductor process is a new field of application of SR, in which studies have been steadily increasing over recent years.¹⁻¹⁸ Etching,^{2,5-9,18} and chemical vapor deposition (CVD)^{1,6,13} including epitaxial growth,^{10,11} doping¹² and surface modifications^{3,4} are especially important applications of SR processes. SR etching using reaction gases such as sulphur hexafluoride (SF₆),^{6,7} chlorine,^{2,8} oxygen⁵

and hydrogen¹⁸ has been reported. Unique material selectivity was found in etching silicon and silicon dioxide (SiO₂) materials using SF₆.⁶ SiO₂ has been found to desorb¹⁴ or evaporate¹⁵ upon SR irradiation, and potential application of this phenomenon to the low-temperature cleaning of silicon surfaces has been demonstrated.¹⁶ The usefulness of undulator light was demonstrated in investigating wavelength dependence in etching experiments using SF₆.⁷ In CVD experiments, the possibility of patterned deposition using a masked SR source was demonstrated.^{1,13} The silicon surface was found to be nitrified by SR irradiation under ammonia (NH₃) gas at low temperatures.^{3,4} Successful SR-assisted low-temperature epitaxial growth was achieved on silicon¹⁰ and metal films.¹¹ Furthermore, potential application of SR to area-selective monolayer processes was also demonstrated in silicon epitaxial growth¹⁷ and boron doping.¹²

Surface reaction dynamics induced by core¹⁹ or valence²⁰ electron excitation are very interesting from the scientific viewpoint, in the study of SR photochemical reactions. Chemical reactions induced by electronic excitations have been studied through the use of electron beams or ion beams. With these excitation sources, however, excitation energy cannot be monochromatized and sputtering effects often lead to complex reaction mechanisms. The reaction models proposed by Knotek-Feibelman (KF)¹⁹ and Menzel-Gomer-Redhead (MGR)^{20a,b} have been known to be useful in explaining stimulated desorption phenomena induced by core and valence electron excitations, respectively. Monochromatized SR beams may be the most excellent excitation source for a more detailed study of these phenomena or to study more complex relaxation processes, including chemical reactions between excited atoms and surrounding molecules.

X-ray lithography has been studied for over ten years as an important application of SR in the

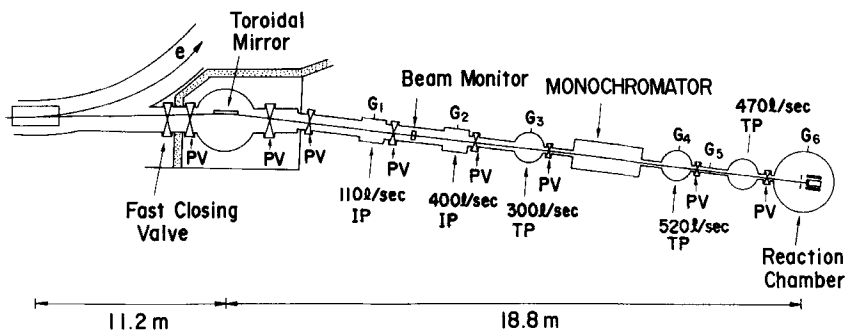


Figure 1 Schematic diagram of beamline BL-1C and reaction chamber. IP, Ion pump; TP, turbo molecular pump; PV, pneumatic valve; G_i , cold cathode vacuum gauge. Volumetric flow rates are in $\text{dm}^3 \text{s}^{-1}$ (l/sec).

fields of semiconductor fabrication. Furthermore, storage rings for the purpose of this industrial application have been constructed in recent years.²¹ Considering that storage ring facilities are fairly expensive despite usually being able to provide more than ten beam ports, it is extremely important, from the viewpoint of efficiency, to develop new fields of application other than X-ray lithography.

Many studies have been reported on photo-excited processes using lasers²²⁻²⁶ or discharge lamps.²⁷ Some of these projects have successfully found practical applications, such as the repair or wiring of semiconductor tips. However, since many reaction gases used in semiconductor processes have large electronic excitation cross-sections in the vacuum ultraviolet (VUV) region with energy higher than about 10 eV, the lasers or discharge lamps usually available cannot excite, or they require high power to excite, these molecules; this is inevitably accompanied by thermal effects. In contrast, SR can excite all of the reaction gases efficiently, and can induce almost pure photochemical reactions with negligible thermal effects.

Temperature lowering in semiconductor processes is now recognized to be an indispensable requisite in the fabrication of future devices, such as quantum effect devices. For example, it has been pointed out that epitaxial growth temperatures less than 300 °C are required to keep the abruptness of silicon/germanium heterojunctions.²⁸ These are extremely severe conditions, considering that epitaxial growth of silicon by CVD is conventionally achieved at substrate temperatures higher than 700 °C. In recent years, it has been found that epitaxial growth temperatures can be significantly lowered by the ultrahigh-vacuum (UHV) CVD method.²⁹

However, this method is not yet developed sufficiently to satisfy the above conditions. The SR-excited process is a promising technique in this direction because of its low-temperature, low-damage and low-contamination process characteristics.

This report reviews recent results of our experiments with SR etching and CVD, aiming at applications to low-temperature semiconductor processes. Reaction models are given and peculiar characteristics of SR processes are discussed based on these experimental results.

2 EXPERIMENTAL SYSTEMS

In the VUV range useful for photochemical reaction, we do not have any sufficiently transparent window material. Because of this, the difference in pressure between the reaction chamber using reaction gases and the high vacuum of the beam line is sustained by differential vacuum pumping.^{30,31} Another important parameter of the beam line is horizontal beam divergence of the emitted SR beam. Photon flux is in proportion to the usable beam divergence. Differential vacuum pumping usually requires a small-diameter beam line duct. This limits usable beam divergence. Large divergence expands the size of the beam spot at the focusing point due to astigmatism. The size of the focusing or reflecting mirror, or the diameter of the beam output port of the SR ring, also limit usable beam divergence. In this context, an undulator, emitting an intense beam with high directivity, is claimed to be ideal in studying photochemical reactions.^{7,32}

Figure 1 shows a schematic diagram of beam line BL-1C and the reaction chamber set up at the

Photon Factory of the National Laboratory for High Energy Physics (KEK), which was constructed for the study of photochemical processes.³⁰ The electron beam energy of the storage ring is 2.5 GeV. At the entrance port of the reaction chamber, the vacuum gradient is about two orders of magnitude over a distance of about 18 cm. The emitted beam, with 2 mrad of horizontal beam divergence, is reflected by a toroidal mirror with a grazing incident angle of 4° and focused into the reaction chamber. The calculated spectrum of the beam is distributed continuously from 1 nm to over 100 nm with a peak around 10 nm. The power of the beam was about 0.7 W for 100 mA of ring current.

Figure 2 shows the reaction chamber settled at the end of the beam line. It is designed as the gas source molecular beam epitaxial (MBE)³³ apparatus to study SR surface cleaning and epitaxial growth of silicon. Base pressure pumped by a 1000 dm³ s⁻¹ turbo molecular pump was 5 × 10⁻¹⁰ Torr. The substrate was heated from the rear with a thin-film carbon heater. Substrate temperature was monitored by a thermocouple gauge attached to the rear of the substrate. Observed values were corrected by a calibration curve previously determined from the surface-temperature monitor.

3 CLASSIFICATION OF SR-EXCITED SURFACE PHOTOCHEMICAL REACTIONS

Surface photochemical reactions in deposition and etching are classified in regard to excitation mechanism as shown in Table 1.³⁴ Here, the

surface excitation mechanism is especially important, since many useful effects of irradiation, unobtainable by other techniques, are expected.

The initial processes of SR excitation are categorized into valence electron excitation and core electron excitation.³⁵ In the former, a localized valence hole (one hole) state with lifetime τ is generated first. It then relaxes to a stable or metastable state (reaction product M) with a yield $P(\tau)$. The reaction cross-section σ_{vr} is given by $\sigma_{vr} = \sum \sigma_{vi} P_i(\tau)$, where σ_{vi} is the excitation cross-section from the ground state to the valence hole state i . With core electron excitation, a core hole state is generated first. Then, with a certain fraction f_D , a localized valence hole (two or three holes) state is generated through Auger processes, and the valence hole state relaxes to reaction product M with a yield $P(\tau)$. Thus, the reaction cross-section σ_{cr} is given as $\sigma_{cr} = \sum \sigma_{ci} f_{Di} P_i(\tau)$.³⁵

Next, the reaction rate is considered in the case of the surface excitation mechanism (Table 1, I–IV). In the following discussion, typically occurring simple cases, for example first-order reactions with reacting species, are considered without further specifications. Rate equations used for both deposition and etching are derived as follows.³⁴

$$\frac{dN_{A'}}{dt} = k_a \Gamma(N_0 - N_{A'}) - k_d N_{A'} - k_t N_{A'} - k_p I_p N_{A'} \quad [1]$$

$$R = k_p I_p N_{A'} + k_t N_{A'} \quad [2]$$

$$k_x = C_x e^{-E_x/RT} \quad [3]$$

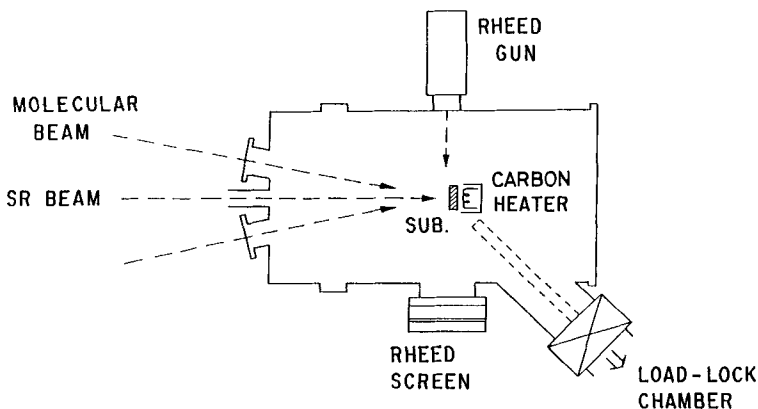
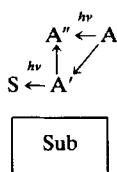
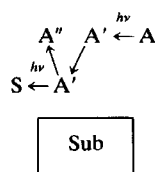
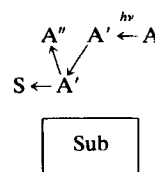
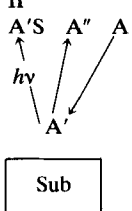
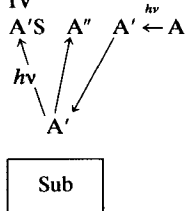
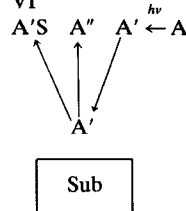


Figure 2 Reaction chamber designed as a gas source MBE system. SUB, substrate.

Table 1 Classification of surface photochemical reactions

Process	Surface excitation	Surface + gas-phase excitation	Gas-phase excitation
Deposition	I 	III 	V 
Etching	II 	IV 	VI 

A, gas molecule; A', adsorbed molecule; A'', desorbed molecule; S, deposited molecule; A'S, etching product; Sub, substrate.

where $N_{A'}$ is the surface density of adsorbed species A', and N_0 is the surface density of adsorption sites at $N_{A'}=0$, Γ is the surface collision frequency of A, and I_p is the photon flux. Each term in Eqn [1] corresponds to adsorption, desorption, thermal reaction and photo-excited reaction, in the order from left to right. Reaction rate R in the stationary state for the generation of S or A'S (in Table 1) is given by

$$R = \frac{k_p k_a \Gamma I_p N_0 + k_t k_a \Gamma N_0}{k_a \Gamma + k_d + k_t + k_p I_p} \quad [4]$$

The photo-excitation reaction term $R_p = k_p I_p N_{A'}$ is now considered in detail. It is convenient to consider the following two cases.

Case 1: A direct photo-excitation process, where valence hole state (h) relaxes directly to reaction product M.

Case 2: A photo-assisted process, where metastable reactive state (*) is firstly generated from valence hole state (h), then reaction product M is generated by reaction between the metastable reactive state and, as an example, adsorbed species A'.

The rates for both cases are given by:

Case 1:

$$\frac{dN_{A'h}}{dt} = I_p N_{A'} \sigma - \frac{N_{A'h}}{\tau_b} - \frac{N_{A'h}}{\tau_m} \quad [5]$$

$$R_p = \frac{1/\tau_m}{1/\tau_b + 1/\tau_m} \sigma I_p N_{A'} \quad [6]$$

Case 2:

$$\frac{dN_{A'h}}{dt} = I_p N_{A'} \sigma - \frac{N_{A'h}}{\tau_b} - \frac{N_{A'h}}{\tau_r} \quad [7]$$

$$\frac{dN_{A'^*}}{dt} = \frac{N_{A'h}}{\tau_r} - \frac{N_{A'^*}}{\tau_f} - k_m N_{A'^*} \quad [8]$$

$$R_p = \frac{1/\tau_r}{1/\tau_b + 1/\tau_r} \frac{k_m}{1/\tau_f + k_m} \sigma I_p N_{A'} \quad [9]$$

where $N_{A'h}$ and $N_{A'^*}$ are surface densities of adsorbed species A' in the valence hole state and metastable reactive state, respectively; $1/\tau_m$ expresses the rate for the valence hole state to relax to product M, and $1/\tau_b$ represents all other relaxation routes. Similarly, $1/\tau_r$ represents the rate for the valence hole state to generate the metastable reactive state, and $1/\tau_b$ is that for all other routes. Reaction constant k_m is defined for

the thermal reaction between the metastable reactive state and N_A , and $1/\tau_i$ is defined for all other routes. The σ in Eqns [5] and [7] is the same as σ_i in valence electron excitation, and $\sigma_{c/Di}$ in core electron excitation. Similarly, $P_i(\tau)$ is given by equations including τ_x and k_m in Eqns [6] and [9]. For both Cases 1 and 2, adsorbed species are considered as excited. Substrate surface excitation is also formulated in a similar manner.

4 ETCHING

4.1 Etching through reaction gas and material selectivity

It was found that silicon and SiO_2 are etched by SR irradiation using reaction gas SF_6 .⁶ Two kinds of reaction mechanisms are observed, namely surface excitation and gas-phase excitation mechanisms. The gas-phase excitation mechanism is a similar one to that observed in plasma etching, where etching proceeds through the thermal reaction between F radicals produced in the gas phase or on the substrate surface. Figure 3 shows the observed etching profiles for SiO_2 , polysilicon (poly-Si) and crystalline Si (c-Si).³⁶ With SiO_2 , the etching profile agrees with the beam intensity profile, indicating that only the surface excitation mechanism is dominant. Both gas-phase and surface excitation mechanisms contribute to poly-Si etching. The gas-phase excitation has been found to be quenched by adding a small percentage of oxygen to the SF_6 .³⁶ The rate of etching on c-Si almost vanishes on addition of oxygen, indicating that c-Si is etched only through the action of the gas-phase excitation mechanism.^{6,36} This effect of addition of oxygen is explained by the fact that the surface oxide layer or the adsorbed oxygen layer produced through the addition of oxygen protects the surface from the etching reactivity of F radicals. Table 2 shows the material selectivity of the etching rate. It is known that the surface excitation mechanism is observed in the insulators SiO_2 , silicon nitride (Si_3N_4) and poly-Si, but is not observed in c-Si.

It has been found that the dependence on doping of etching rate in poly-Si is quite different from that in plasma etching³⁷ or laser etching.³⁸ For both n- and p-types, the SR etching rate decreases with increasing carrier concentrations, as shown in Fig. 4.^{39,40} For plasma etching using XeF_2 gas, the etching rate of n-type silicon is

larger than that of undoped or p-type silicon, and the rate increases with increasing n-type dopant concentrations.³⁷ In excimer laser etching of c-Si using NF_3 gas, the dependence of etching rate on conductivity is not so significant.

Another important property of etching of poly-Si and amorphous silicon is the dependence of etching rate on beam intensity. For SiO_2 , the etching rate depends linearly on beam intensity, i.e. the etching rate per unit photon flux is constant. However, with poly-Si or amorphous silicon, it has been found that etching rate per unit photon flux increases with increasing beam intensity, as shown in Fig. 5.⁴⁰

The material selectivity in the gas-phase excitation mechanism may reflect the difference in the reactivity of the F radical on the substrate surface. Material selectivity in the surface excitation mechanism can be summarized as follows.⁴⁰

- (1) Insulating materials are etched at a higher rate than semiconducting materials.
- (2) The etching rate of silicon depends on its crystallinity. Crystalline silicon cannot be etched by the surface

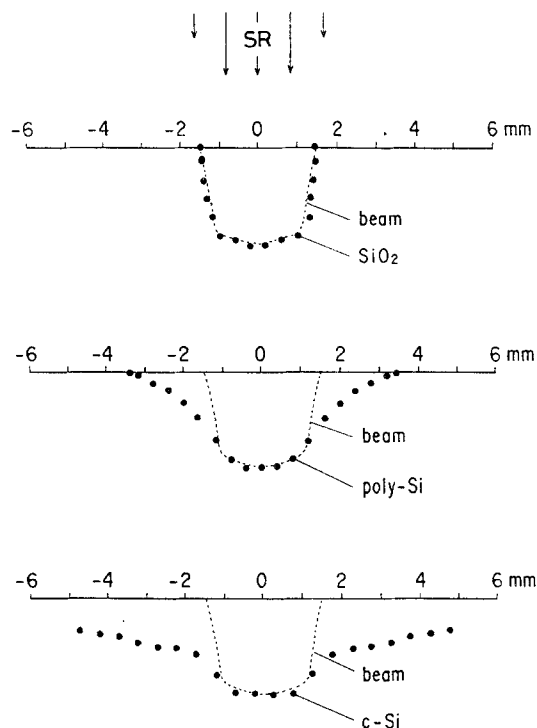


Figure 3 Observed etching depth profiles of SiO_2 , poly-Si and c-Si without oxygen addition, together with SR beam intensity distribution. Pressure of SF_6 was 0.08 Torr for SiO_2 , poly-Si and c-Si etching. Average ring current of the storage ring was 270 mA during experiments. (From Ref. 36.)

Table 2 Material selectivity of etching rate, normalized to a ring current of 100 mA and irradiation time 1 min

Material	SF ₆ (Å)	SF ₆ + O ₂ (Å)
SiO ₂	19.5	19
Si ₃ N ₄	28.3	15–19
Poly-Si	18	8
n-type c-Si	14.5	0

excitation mechanism. The etching rate of silicon increases with degradation in crystallinity. (3) The etching rate of poly-Si or amorphous silicon also depends on conductivity. Etching rate decreases with increasing conductivity. Figure 6 shows the line and space pattern fabricated by SR etching using SF₆ + O₂ (10%) gases. A poly-Si thin film with the line and space pattern fabricated by electron beam lithography was used as the etching mask. Etching stops completely at the c-Si surface.

Figure 7 shows the dependence of etching rates of SiO₂ and poly-Si on temperature. This temperature dependence indicates that the rate-determining step in the reaction is the direct photo-excitation process. Material selectivity is

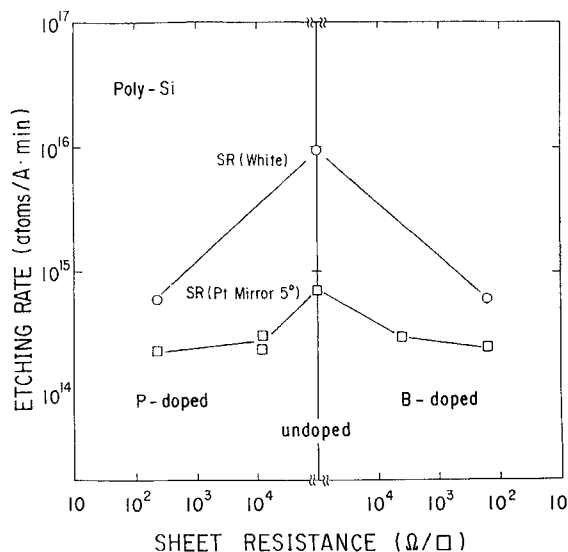


Figure 4 Etching rate of poly-Si as a function of sheet resistance controlled by P or B doping concentrations under conditions of SF₆ total pressure 0.08 Torr, substrate temperature 300 K and storage ring current 170 mA. Two kinds of beam line optics were used: the system with only one toroidal mirror and the system with one toroidal mirror and a pair of platinum-coated plane mirrors with grazing incidence angle of 5°. (From Ref.39.)

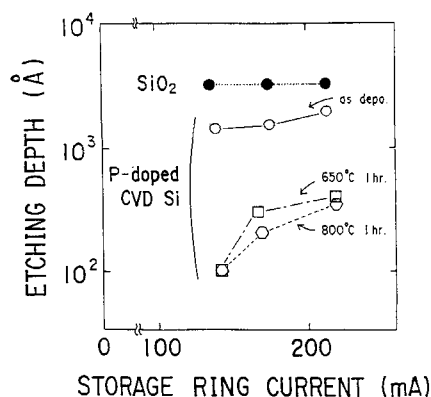


Figure 5 Etching rate of SiO₂, P-doped poly-Si and amorphous silicon as a function of storage ring current for a constant dose, 2.2×10^4 mA min (ring current \times etching time). P-doped CVD silicon was amorphous as deposited, and polycrystalline after annealing at 650 °C or 800 °C (From Ref. 40.)

qualitatively explained by assuming that the reactive centre, which is the valence hole state itself or some state generated through the relaxation of the valence hole state, is easily quenched in c-Si or highly conductive poly-Si before the fluorination reaction occurs. On the other hand, in insulating materials or low-conductive poly-Si, the lifetime of such a reactive center is sufficiently long to induce the fluorination reaction and desorption of SiF_n.

4.2 Etching without reaction gas

It has been found that SiO₂ evaporates at relatively low temperatures on SR irradiation under UHV conditions.¹⁵ Figure 8 shows a photograph of the SR-irradiated portion of a thermal oxide

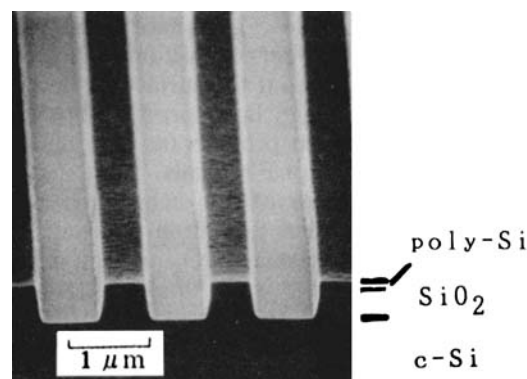


Figure 6 Line and space etched pattern. Poly-Si film preliminarily patterned by electron beam lithography was used as an etching mask. Reaction gas was SF₆ + O₂ (10%). Ring current was about 200 mA. Irradiation time was about 2 hours.

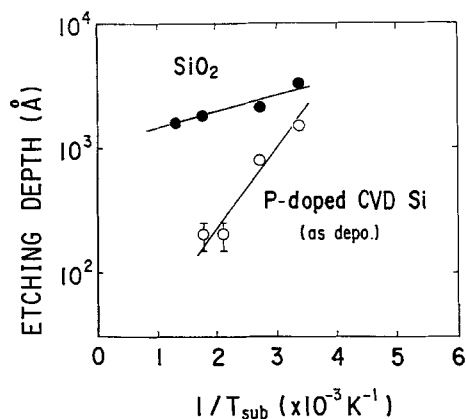


Figure 7 Dependence of etching rate on substrate temperature. Dose was 2.2×10^4 mA min. SF_6 pressure was 0.13 Torr.

film grown on an Si(100) substrate, where SiO_2 has evaporated out exposing metallic silicon surface. The evaporation rate increases gradually with increasing temperature, and the rate of increase becomes much larger above 500°C , as shown in Fig. 9. Important features of this phenomenon are the following. Evaporation occurs only on irradiated areas, with a spatial resolution of less than a few tens of nanometers. Moreover, it has material selectivity in that neither polycrystalline nor crystalline silicon are evaporated.

It is noteworthy that effective activation energy gradually increases with increasing temperature. It is roughly evaluated to be $17.7 \text{ kcal mol}^{-1}$ (74 kJ mol^{-1}) and $5.2 \text{ kcal mol}^{-1}$ (22 kJ mol^{-1}) above and below 450°C , respectively. In the higher temperature region, the mechanism $\text{SiO}_2 \rightarrow \text{SiO}^*(\text{s}) + \frac{1}{2}\text{O}_2^*(\text{s})$ by core and valence electron excitation, followed by $\text{SiO}^*(\text{s}) \rightarrow \text{SiO}(\text{g})$ and $\text{O}_2^*(\text{s}) \rightarrow \text{O}_2(\text{g})$, is proposed by Nishiyama,

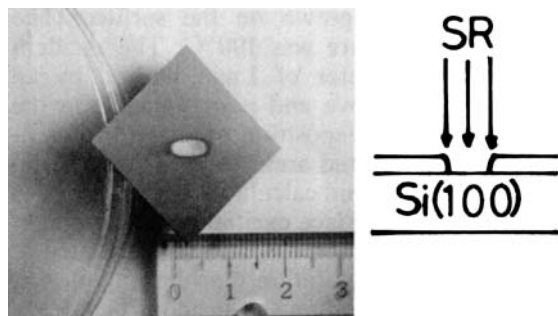


Figure 8 Photograph of an SR-irradiated part of an SiO_2 film thermally grown on Si(100) substrate. The SiO_2 film is evaporated by SR irradiation.

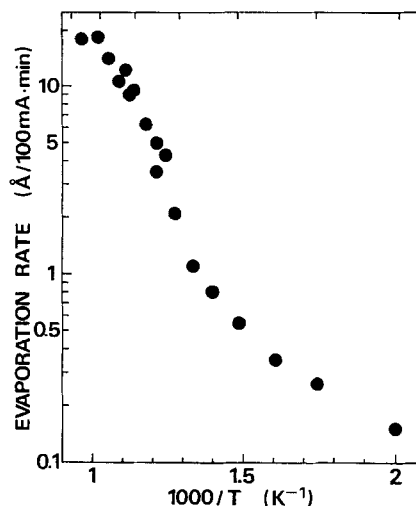


Figure 9 Dependence of SiO_2 evaporation rate for a ring current of 100 mA on substrate temperature T . (From Ref. 15.)

based on the detection of desorbed SiO and O_2 .⁴¹ Contribution of many kinds of metastable species is a possible explanation for the gradual change of activation energy.

Thermal evaporation of SiO_2 is used as a conventional surface cleaning method for silicon substrates.⁴² Therefore, SR evaporation of SiO_2 is expected to be applicable to low-temperature surface cleaning.¹⁶ Figure 10 shows RHEED patterns observed on the surface after 6 h of SR irradiation at 650°C on an Si(100) substrate with native oxide formed on its surface by the wet method. The figure also shows the surface after Si epitaxial growth on the SR-irradiated part of the substrate with Si_2H_6 under 2×10^{-5} Torr. It is clear that a 2×1 reconstruction pattern is observed for both surfaces after cleaning and epitaxial growth, indicating the cleanliness and good crystal quality.

4.3 Boundary effects in etching

The above experiments indicate that the SR evaporation phenomena can, in principle, be applicable to the surface cleaning of silicon substrates in a treatment for silicon epitaxial growth. However, it must be noticed that the cleaning time is anomalously long compared with the time estimated from the evaporation rate for bulk SiO_2 (shown in Fig. 9) and the thickness of native oxide, usually less than 20 \AA (2 nm). This indicates that either the evaporation rate of a thin

SiO₂ film on c-Si is slow compared with that of thick SiO₂, or it slows down near the SiO₂/Si boundary. A similar phenomenon has been considered to exist in etching with SF₆ gas. The etching rate of c-Si is decreased to almost zero by adding oxygen to SF₆.^{6,36} This effect in the unirradiated area is explained by the formation of a surface oxide layer protecting the silicon surface from the etching reaction by F radicals generated by gas-phase excitation. The disappearance of etching rate in the irradiated area, however, cannot simply be explained by this mechanism, since it is known that bulk SiO₂ is easily etched by the surface excitation mechanism. This contradiction is also explained, if the etching rate of a thin SiO₂ film on c-Si is assumed to be much slower than that on bulk SiO₂. This also applies to SF₆ etching. Bearing in mind material selectivity, that the etching rate of Si decreases with either increasing conductivity or crystallinity, and also the related reaction model described above, one possible explanation for these boundary effects is that the lifetime of reactive centers generated close to the substrate surfaces by SR irradiation is shortened due to the influence of substrate c-Si.

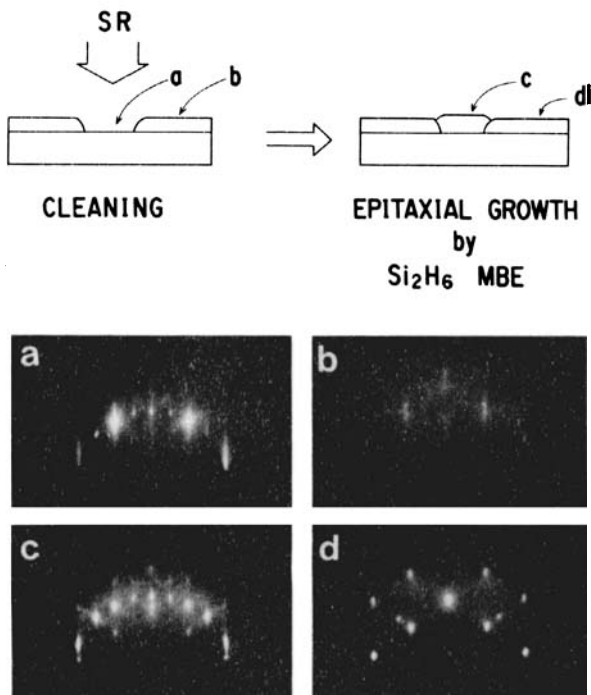


Figure 10 RHEED patterns observed after SiO₂ evaporation (a, b) and Si epitaxial growth (c, d). The irradiated parts are a and c, and the non-irradiated parts are b and d.

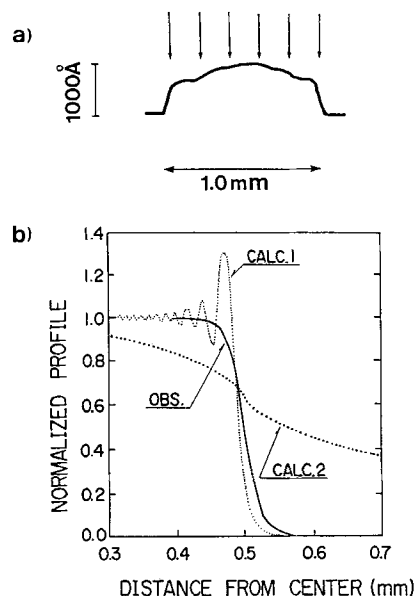


Figure 11 (a) Pattern profile of deposited silicon nitride film. (b) Comparison of observed profile with profiles calculated on the basis of the surface-excitation mechanism (CALC.1) and the gas-phase excitation mechanism (CALC.2).

5 SR-EXCITED CVD OF Si_xN_yH_z FILM

Hydrogen-containing silicon nitride film is used as a passivation film in metal-organic semiconductor field effect transistors (MOSFETs). In this application, it has been reported that the hydrogen contained in the film causes some degradation of the transistors.⁴³ Since surface hydrogen is desorbed efficiently by SR excitation, it is expected that the hydrogen content of the CVD film is reduced by SR irradiation.

Figure 11 shows the pattern profile of a silicon nitride film deposited by SR CVD using SiH₄ (0.02 Torr) and nitrogen (0.1 Torr) as a reaction gas.^{1,6} Substrates were silicon wafers with SiO₂ film 100 nm thick grown on the surface. The substrate temperature was 190 °C. The incident beam had a diameter of 1 mm limited by an orifice set 1 cm above and perpendicular to the substrate surface. Deposition occurred preferentially on the irradiated area. From a comparison between observed and calculated edge profiles, it is concluded that surface excitation is a dominant mechanism. Deposition can also be attributed in part to gas-phase excitation mechanism, since it was observed even when the incident beam was parallel to the substrate surface, although the rate was slower than for the perpendicular arrangement. The hydrogen content of the deposited film

was determined from the infrared absorption spectrum. Figure 12 shows the dependence of hydrogen content on the composition (N/Si).⁶ The reported values of the hydrogen content in a mercury-lamp-excited CVD film⁴⁴ and in a plasma CVD film⁴⁵ are given in the same figure. Silicon nitride films with a relatively low hydrogen content can be obtained with SR CVD.

It is interesting to compare nitrogen (N₂) and ammonia (NH₃) gases as nitrogen sources, since NH₃ is an extremely adsorptive gas. Figure 13 shows the dependence of film composition on partial pressure ratio R_p of the reaction gas.^{46,47} With the (SiH₄+NH₃) system, film composition suddenly increases at around $R_p = P_{NH_3}/P_{SiH_4} = 1$ and saturates slightly above the stoichiometric value. On the other hand, with the (SiH₄+N₂) system, the efficiency of nitrogen incorporation is low and composition (N/Si) increases in proportion to R_p . Saturation at around N/Si = 1 is due to the attenuation of incident beam intensity by the absorption by the reaction gas. Concerning the sudden increase of film composition, it has been found that the detailed behavior of the increasing curve shows characteristic differences among the substrate materials as shown in Fig. 14.^{46,47} The sudden increase occurs at a higher value of R_p in crystalline silicon substrates than in Si₃N₄. In the case of SiO₂ substrates, a curve similar to that of the Si₃N₄ was obtained. This nonlinear behavior of the composition and its dependence on the substrate material can be qualitatively explained by considering that the efficiency of nitrogen incorporation is higher in insulating materials than in semiconducting materials. Here it must be

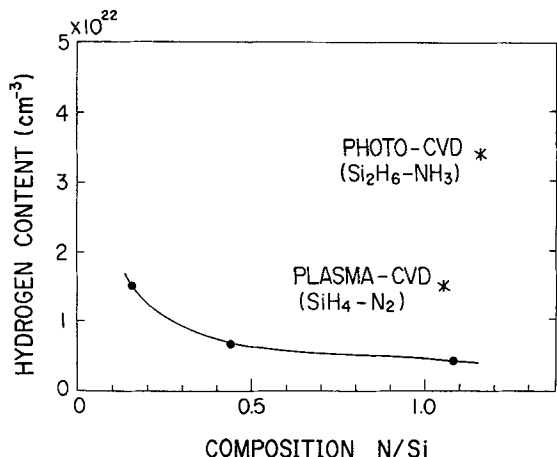


Figure 12 Dependence of hydrogen content on the N/Si composition of deposited Si_xN_yH_z film. Substrate temperature was 190 °C.

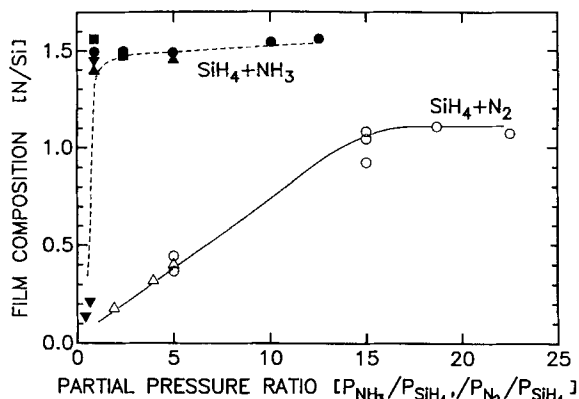


Figure 13 Relationship between film composition and partial pressure ratio. Substrate temperature was 200 °C. Pressure of SiH₄ was 2×10^{-2} (○, ●), 3×10^{-2} (△, ▲), 5×10^{-2} (■), and 0.1 Torr (▼). (From Ref. 46.)

noticed that the ‘substrate material’ changes during the progress of deposition, since deposition itself changes the condition of the substrate surface. Therefore, with insulating substrates, the deposited film is a semiconductor with low R_p values, but changes to an insulator at around $R_p = 0.8$, accompanied by an increase in the efficiency of nitrogen incorporation. It is reported that SiN_x:H film changes from a semiconductor to an insulator at around $x = 0.3$.⁴⁸ With c-Si substrates, nitrogen incorporation

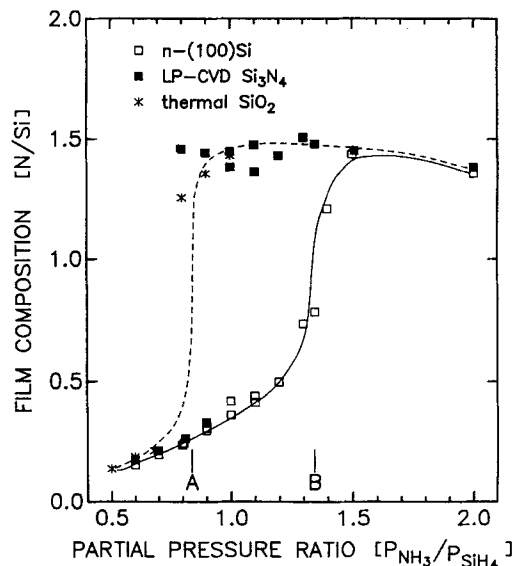


Figure 14 Relationship between film composition and partial pressure ratio for Si₃N₄ and c-Si substrates. Substrate temperature was 200 °C. Si₂H₆ pressure was 1.2×10^{-4} Torr. (From Ref. 46.)

efficiency is low at the initial stage of deposition. Therefore, it is easily understood that the deposited film changes from a semiconductor to an insulator at a relatively larger value of R_p . Here, it should be remembered that similar material selectivity is observed in etching reactions using SF_6 . Therefore, electronic excitation of the substrate surface is considered to induce the nitridation reaction of silicon in the $(SiH_4 + NH_3)$ system.

6 SR EXCITED EPITAXIAL GROWTH OF SILICON

It has been pointed out that the temperature of silicon epitaxial growth in CVD is limited by the stability of silicon oxide formed by reaction with residual O_2 or H_2O , and that a fairly low temperature (500–700 °C) epitaxial growth (low-temperature limit in thermal reaction) is achieved by UHV-CVD.²⁹ The main interest in this section is to see whether SR irradiation affects epitaxial growth at the low-temperature limit of the thermal reaction.

A reaction gas of 100 % Si_2H_6 was fed into the reaction chamber shown in Fig. 2. The Si(100) substrates were used and surface cleaning was achieved by the conventional thermal desorption method. Native oxide was prepared by the wet method.⁴²

The observed dependence of growth rate on temperature is shown in Fig. 15.¹⁰ The reaction gas pressure was 1.5×10^{-4} Torr. Temperature dependence apparently shows the presence of two regions. In the higher temperature region, the effects of SR irradiation on growth rate are not observed. However, at temperatures lower than 600 °C, growth rate due to SR irradiation increases with decreasing temperature. Good crystal quality was assured by the 2×1 RHEED pattern measured just after the growth, as shown in Fig. 16, for all experimental samples. Therefore, the results in Fig. 15 indicate that SR irradiation greatly improves the low-temperature limit of epitaxial growth of silicon by UHV-CVD.

The temperature dependence of epitaxial growth of silicon shows that this reaction is the sum of the photo-assisted process and the thermal process. Deposition rate is characterized by Eqns [4] and [9]. Temperature dependence can be separated into two regions at about 600 °C. Similar dependences are observed in UHV-CVD using SiH_4 .^{49,50} In the higher temperature region,

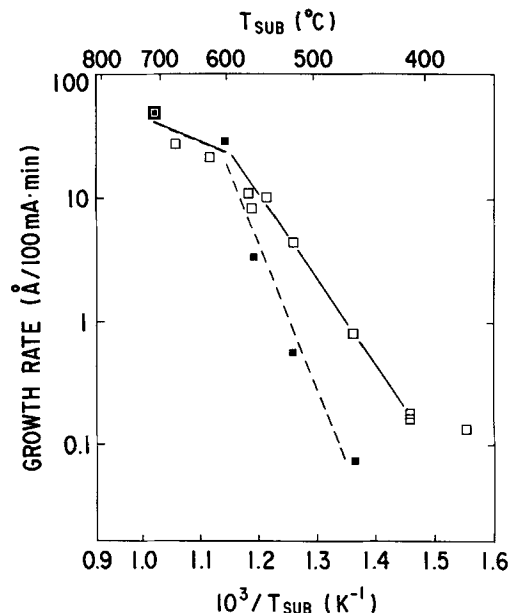


Figure 15 Dependence of epitaxial growth rate of silicon on substrate temperature for both thermal (■) and SR irradiation (□) processes. (From Ref. 10.)

the thermal reaction constant (k_t) becomes large, so the deposition rate is given by $R = k_a \Gamma N_0$, indicating that chemisorption is the rate-limiting process. Concerning the low-temperature region, activation energies are determined to be 31 kcal mol^{-1} (130 kJ mol^{-1}) with SR irradiation and 54 kcal mol^{-1} (226 kJ mol^{-1}) without it, from the data of Fig. 15. Without SR irradiation, since term k_a is larger than k_t , the deposition rate is given by $R = k_t N_0$. This means that the thermal reaction is rate-limiting. For this thermal reaction, hydrogen desorption such as $SiH_2(s) \rightarrow$

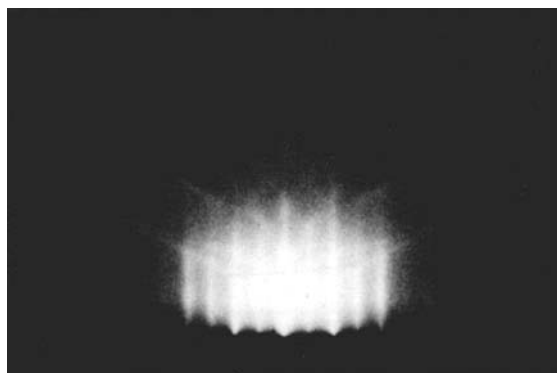
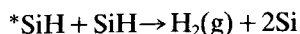


Figure 16 RHEED pattern of an as-grown film deposited on an Si(100) surface at 520 °C ([100] incidence). Si_2H_6 pressure was 1.5×10^{-4} Torr.

$\text{Si(s)} + \text{H}_2(\text{g})$, $E_t = 59 \text{ kcal mol}^{-1}$ (247 kJ mol^{-1}),⁵¹ is considered as an example.

The deposition rate under SR irradiation is given in the form $R = k_p I_p N_0$. Photo-assisted hydrogen desorption, such as



is considered to be a mechanism operative under SR irradiation effects.

For both SiO_2 evaporation and epitaxial growth, further experiments, such as observation of desorption species, are necessary to understand correctly the reaction mechanism. However, it is believed that the present analysis explains well the temperature dependences of these phenomena qualitatively or semiquantitatively. Therefore, from the present experimental data and analysis, it is concluded with certainty that the SR photochemical reaction can provide a new low-temperature process overcoming the low-temperature limit of the thermal process.

7 APPLICATION TO ATOMIC LAYER PROCESS

Atomic layer epitaxial (ALE) growth is expected to be an important technique in such applications as the fabrication of superlattice structures and surface or interface modifications.⁵²⁻⁵⁵ It is also interesting as a reaction system to study the relationship between epitaxial crystal growth and substrate temperature. One established way to attain ALE is to find a molecule with self-limiting adsorption on the substrate surface and then find a method to release this self-limiting function and reactivate the surface for adsorption. The second process usually requires desorption of the group which prevents succeeding adsorption. Thermal desorption is the conventional method. However, temperatures higher than 500°C are usually required for thermal desorption, which often destroy the structure of the atomic layer itself. Therefore, as a low-temperature process, photo-stimulated desorption is considered to be the most promising technique, especially the use of VUV photons to excite the electronic states of all molecules efficiently.

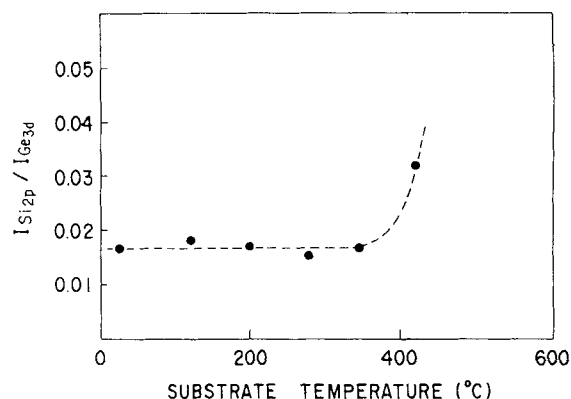


Figure 17 Dependences of XPS intensity ratio between Si_{2p} and Ge_{3d} on substrate $\text{Ge}(100)$ temperature. Exposure to SiH_2Cl_2 gas is $1.1 \times 10^7 \text{ dm}^3$ ($0.09 \text{ Torr} \times 120 \text{ s}$). (From Ref. 17.)

The dependence of the degree of adsorption of SiH_2Cl_2 on the substrate temperature was evaluated on the clean surface of a germanium substrate by using X-ray photoelectron spectroscopy (XPS). It was found that the stable self-limiting adsorption is kept at temperatures lower than about 400°C , as shown in Fig. 17.¹⁷ Since the Cl atom is observed as the thermal desorption species from this self-limiting adsorption surface of SiH_2Cl_2 ,¹⁷ the reaction in the self-limiting adsorption is considered to be expressed by



where (gas) and (ad) represent the gas phase and adsorption state, respectively. Since it is known that atom mixing at the silicon and germanium layer interface starts to occur at about 300°C ,²⁸ the photo-stimulated desorption is considered best for silicon/germanium systems.

Figure 18 shows Auger electron (AE) spectra of the surface of a germanium substrate after six cycles of the layer-by-layer process at 300°C using SR irradiation.¹⁷ Each cycle consists of three procedures: (1) SiCl_2H_2 gas exposure of $1.1 \times 10^7 \text{ L}$ ($6 \times 10^{-2} \text{ Torr}$, 180 s) without SR irradiation; (2) 1 min evacuation pumping to less than 10^{-7} Torr ; and (3) 10 min SR irradiation. Spectra (a) and (b) correspond to irradiated and non-irradiated areas, respectively. Four to five times as many Si atoms are deposited on the irradiated area as on the non-irradiated area. In comparison with the AE spectra measured for a thick silicon film deposited by continuous SR irradiation and for the Ge substrate, it has been determined that the

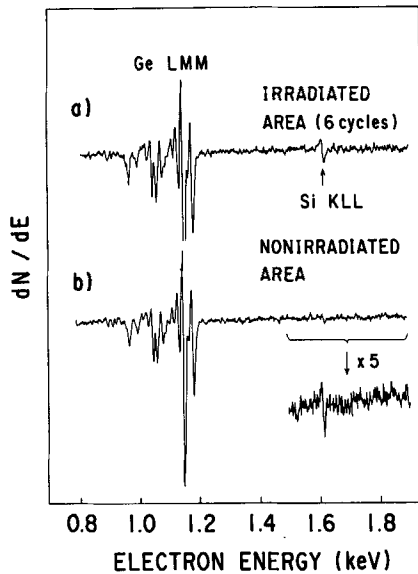


Figure 18 Observed AE spectra for (a) SR-irradiated area and (b) non-irradiated area on Ge(100) surface after six cycles of the layer-by-layer process.

signal intensity of the silicon KLL transition in the spectrum (a) corresponds to three to five atomic layers. The RHEED pattern for the irradiated area after deposition was the same as the 2×1 reconstruction pattern observed just after cleaning the germanium substrate. The results indicate that SR irradiation breaks the self-limiting property of the SiCl_2 -adsorbed surface at a sufficiently low temperature. Therefore, it is concluded that the sequential process of self-limiting adsorption of SiH_2Cl_2 and SR irradiation holds promise of success for developing the silicon ALE technique.

Acknowledgements The authors would like to thank co-workers of their research group—Hakaru Kyuragi, Yasuo Takahashi and Izumi Kawashima—for their collaboration in writing this review. Thanks are also given to Tetsushi Sakai for his continuous guidance and encouragement. They also wish to thank the staff at the Photon Factory of the National Laboratory for High Energy Physics (KEK) for their collaboration in these experiments.

REFERENCES

1. Kyuragi, H and Urisu, T *J. Appl. Phys.*, 1987, 61: 2035
2. Hayasaka, N, Hiraya, A and Shobatake, K *Jpn. J. Appl. Phys.*, 1987, 26: L1110
3. Cerrina, F, Lai, B, Wells, G M, Wiley, J R, Kilday, D G and Margaritondo, G *Appl. Phys. Lett.*, 1987, 50: 533
4. Lai, B, Nachman, R, Ray-Chaudhuri, A K and Cerrina, F *Solid State Commun.*, 1989, 71: 721
5. Kyuragi, H and Urisu, T *Appl. Phys. Lett.*, 1987, 50: 1254
6. Urisu, T and Kyuragi, H *J. Vac. Sci. Technol.*, 1987, B5: 1436
7. Shobatake, K, Ohashi, H, Fukui, K, Hiraya, A, Hayasaka, N, Okano, H, Yoshida, A and Kume, H *Appl. Phys. Lett.*, 1990, 56: 2189
8. Terakado, S, Nishino, J, Morigami, M, Harada, M, Suzuki, S, Tanaka, K and Chikawa, J *Jpn. J. Appl. Phys.*, 1990, 29: L709
9. Takahashi, J, Utsumi, Y and Urisu, T *Extended Abstracts of the 20th (1988 International) Conference on Solid State Devices and Materials, Tokyo, 1988*, p 73
10. Takahashi, J, Utsumi, Y, Akazawa, H, Kawashima, I and Urisu, T *Appl. Phys. Lett.*, 1991, 58: 2776
11. Hochst, H and Engelhardt, M A *J. Vac. Sci. Technol.*, 1990, B8: 686
12. Rosenberg, R A, Perkins, F K, Mancini, D C, Harp, G R, Tonner, B P, Lee, S and Dowben, P A *Appl. Phys. Lett.*, 1991, 58: 607
13. Mancini, D C, Varma, S, Simons, J K, Rosenberg, R A and Dowben, P A *J. Vac. Sci. Technol.*, 1990, B8: 1804
14. Niwano, M, Katakura, H, Takakuwa, H and Miyamoto, N *Appl. Phys. Lett.*, 1990, 56: 1125
15. Akazawa, H, Utsumi, Y, Takahashi, J and Urisu, T *Appl. Phys. Lett.*, 1990, 57: 2302
16. Akazawa, H, Utsumi, Y, Takahashi, J and Urisu, T *Extended Abstracts of the 22nd (1990 International) Conference on Solid State Devices and Materials*, p 1171, Business Center for Academic Society Japan, Sendai, 1990
17. Takahashi, Y and Urisu, T *Jpn. J. Appl. Phys.*, 1991, 30: L209
18. Nara, Y, Sugita, Y, Nakayama, N and Ito, T *J. Vac. Sci. Technol.*, 1991, B9: to be published
19. Knotek, M L and Feibelman, P *J. Phys. Rev. Lett.*, 1978, 40: 964
20. (a) Menzel, D and Gomer, R *J. Chem. Phys.*, 1964, 41: 3311; (b) Redhead, P A *Can. J. Phys.*, 1964, 42: 886
21. Hosokawa, T, Kitayama, T, Hayasaka, T, Ido, S, Uno, Y, Shibayama, A, Nakata, J, Nishimura, K and Nakajima, M *Rev. Sci. Instrum.*, 1989, 60: 1783
22. Ehrlich, D J, Osgood, Jr, R M and Deutsch, T F *IEEE J. Quantum. Electron.*, 1980, QE16: 1233
23. Chuang, T J *J. Vac. Sci. Technol.*, 1981, 18: 638
24. Hanabusa, M *Mat. Sci. Rep.*, 1987, 2: 51
25. Donnelly, V M and McCaulley, J A *Appl. Phys. Lett.*, 1989, 54: 2456
26. Yokoyama, S, Yamakage, Y and Hirose, M *Appl. Phys. Lett.*, 1985, 47: 389
27. Yamada, A, Satoh, A, Konagai, K and Takahashi, K *J. Appl. Phys.*, 1989, 65: 4268
28. Iyer, S S, Pukite, P R, Tsang, J C and Copel, M W *J. Crystallogr. Growth*, 1989, 95: 439
29. Meyerson, B S, Ganin, E, Smith, D A and Nguyen, T N *J. Electrochem. Soc.*, 1986, 133: 1232

30. Urisu, T, Kyuragi, H, Utsumi, Y, Takahashi, J and Kitamura, M *Rev. Sci. Instrum.*, 1989, 60: 2157
31. Janes, J and Lutz, N *Appl. Optics*, 1989, 28: 3327
32. Ortega, J M, Billardon, M, Jezequel, G, Thiry, P and Petroff, Y *J. Phys.*, 1984, 45: 1883
33. Hirose, F, Suemitsu, M and Miyamoto, N *Jpn. J. Appl. Phys.*, 1989, 28: L2003
34. Urisu, T, Takahashi, J, Akazawa, H and Utsumi, Y In: *Proceedings of the First International Forum of Optoelectronic Industry and Technology Development Association, Naha Okinawa, 1991*, p. 48, Optoelectronic Industry and Technology Development Association, Tokyo, Japan
35. Ramaker, D E *J. Vac. Sci. Technol.*, 1983, A1: 1137
36. Utsumi, Y, Takahashi, J and Urisu, T *J. Vac. Sci. Technol.*, 1991, B9: to be published
37. Houle, F A *J. Chem. Phys.*, 1983, 79: 4237
38. Horiike, Y, Hayasaka, N, Sekine, M, Arikado, T, Nakase, M and Okano, H *Appl. Phys.*, 1987, A44: 313
39. Takahashi, J, Utsumi, Y and Urisu, T *Mat. Res. Soc. Symp. Proc.*, 1990, 158: 53
40. Takahashi, J, Utsumi, Y and Urisu, T *J. Appl. Phys.*, 1991, 70: to be published
41. Nishiyama, I In: *Proceedings of the First International Forum of Optoelectronic Industry and Technology Development Association, Naha Okinawa, 1991*, p. 69, Optoelectronic Industry and Technology Development Association, Tokyo, Japan
42. Ishizaka, A and Shiraki, Y *J. Electrochem. Soc.*, 1986, 133: 667
43. Fair, R B and Sun, R C *IEEE Trans. Electron Devices*, 1981, 28: 83
44. Okuhira, H and Shintani, A *Proc. 87th Meeting of Crystal Technology Session in the Japan Society of Applied Physics (in Japanese)*, p 23, The Japan Society of Applied Physics, Tokyo, 1986
45. Wood, T H, White, J C and Thacker, B A *Appl. Phys. Lett.*, 1983, 42: 408
46. Kyuragi, H and Urisu, T *Electrochem. Soc. Proc.*, 1988, 7: 326
47. Kyuragi, H and Urisu, T *J. Electrochem. Soc.* 1991, 138: to be published. This paper was originally presented at the 1987 Fall Meeting held in Honolulu, Hawaii.
48. Kurata, H, Hirose, M and Osaka, Y *Jpn. J. Appl. Phys.*, 1981, 20: L811
49. Liehr, M, Greenlief, C M, Kasi, S R and Offenberg, M *Appl. Phys. Lett.*, 1990, 56: 629
50. Hirose, F, Suemitsu, M and Miyamoto, N *Jpn. J. Appl. Phys.*, 1990, 29: L83
51. Buss, R J, Ho, P, Breiland, W G and Coltrin, M E *J. Appl. Phys.*, 1988, 63: 2808
52. Suntola, T *Extended Abstracts 16th Conf. Solid State Devices and Materials*, p 647, Business Center for Academic Societies Japan, Tokyo, 1984
53. Nishizawa, J, Abe, H and Kurabayashi, T *J. Electrochem. Soc.*, 1985, 132: 1197
54. Takahashi, Y, Ishii, H and Fujinga, K *J. Electrochem. Soc.*, 1989, 136: 1826
55. Takahashi, Y, Sese, Y and Urisu, T *Jpn. J. Appl. Phys.*, 1989, 28: 2387